

GLOBAL OBSERVABLES AT RHIC

A. MILOV

Physics Department, Brookhaven National Laboratory, Upton, NY 11973, USA
E-mail: amilov@bnl.gov

Main characteristics of the charged particle $dN_{ch}/d\eta$ and transverse energy $dE_T/d\eta$ production measured in Heavy Ion collisions at RHIC energies are presented in this article. Transformation of the pseudo-rapidity shape, relation to the incident energy and centrality profile are described in a systematic way. Centrality profile is shown to be closely bound to the number of nucleons participating in the collisions, at the same time an alternative approach to study the centrality behavior is also discussed.

Keywords: Heavy Ion Collisions; Transverse Energy; Charged Particle Production; Centrality

1. Introduction

$dN_{ch}/d\eta$ and $dE_T/d\eta$ production are measured by all RHIC experiments BRAHMS, PHENIX, PHOBOS and STAR. After several years of RHIC operation data available from these experiments allow to determine major dependencies in the global observables behavior in High Energy Heavy Ion Collisions. This knowledge is essential for the understanding of the physics of the Heavy Ions Collisions and for setting the framework in which the study of the underlying Quark-Gluon Plasma phase transition has to be carried out.

2. The shape

The PHOBOS¹ and BRAHMS² experiments at RHIC measure the charged particle distribution in a wide range of pseudo-rapidity. Figure 1 shows $dN_{ch}/d\eta$ for different centralities in $Au + Au$ in the full range of $\sqrt{s_{NN}}$ available at RHIC.

All distribution presented in fig. 1 have approximately a trapezoidal shape with a characteristic parameter y_{beam} equal to $\ln(\sqrt{s_{NN}}/m_N)$, where m_N is the mass of the nucleon. One can define three different regions common to all distributions shown in the figure. The flat top region including mid-rapidity is between $\pm 0.4y_{beam}$, the slope also

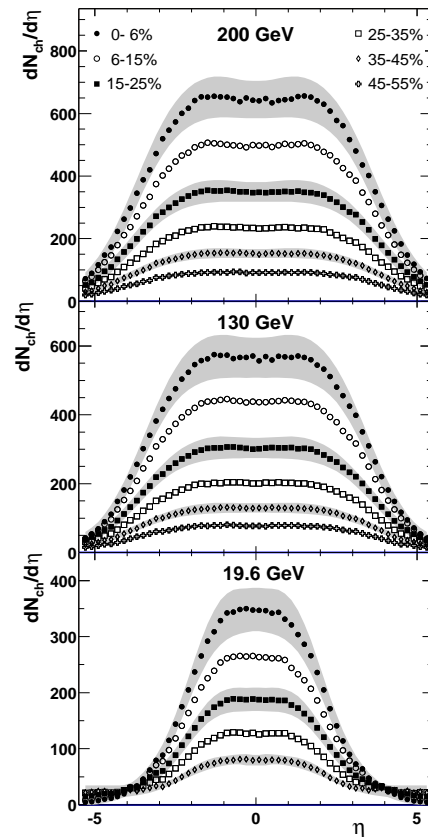


Fig. 1. $dN_{ch}/d\eta$ measured by PHOBOS in a full range of pseudo-rapidity at several RHIC energies.

referred as the Limiting Fragmentation region around $\pm 0.75y_{beam}$ and the Fragmentation region close to $\pm 1.0y_{beam}$ and above.

2

At mid-rapidity where the most particles are produced the distribution increases from peripheral to central collisions as one can see in all 3 panels in fig. 1. Opposite to that in the Fragmentation region $dN_{ch}/d\eta$ decreases when collisions become more central as one can see it in the $\sqrt{s_{NN}} = 19.6 \text{ GeV}$ (lower) panel of the figure.

The Limiting Fragmentation Region located in between of the regions with the opposite trends has a very distinct feature. In the rest frame of the nuclei (in the $\eta - y_{beam}$ frame), the $dN_{ch}/d\eta$ is invariant to the incident energy and to the type of collision species for as long as the centrality of the collisions are the same. This is demonstrated in fig. 2. One shall note that this phenomenon

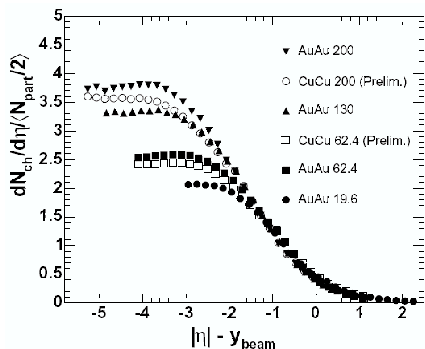


Fig. 2. Limiting Fragmentation Region measured for the same centrality in different collision systems at different $\sqrt{s_{NN}}$.

extends on other collision systems^{3,4} such as $p + p$ and $e + e$ where η and y_{beam} have to be redefined.

3. Incident energy dependence

As it is evident from the figs. 1,2 particle production increases with the incident energy. At the beginning of RHIC operation the PHENIX experiment suggested⁵ that this rise in $dN_{ch}/d\eta$ is $\propto \ln(\sqrt{s_{NN}}/m_0)$ which was later confirmed⁶. Dependence on the incident energy is shown in fig. 3.

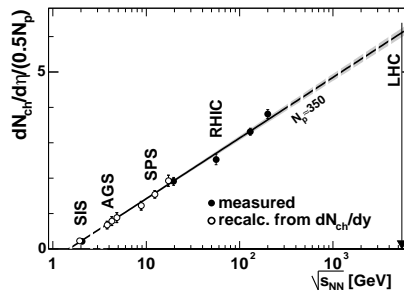


Fig. 3. $dN_{ch}/d\eta$ in the most central collisions as a function of incident energy.

It is interesting to note the the logarithmic dependence holds for more than 2 orders of magnitude in $\sqrt{s_{NN}}$ and work even for a SIS energies^{6,8} where only $\sim 100 \text{ keV}$ kinetic energy is available per nucleon. Assuming the same behavior extends to the LHC energy $\sqrt{s_{NN}} = 5.5 \text{ TeV}$ one would expect to observe ~ 1100 charged particles in the most central events, equivalent to an increase from the highest RHIC energy by $\sim 60\%$.

The amount of the transverse energy produced in $Au + Au$ collisions⁶ also logarithmically depends on $\sqrt{s_{NN}}$. A small difference in m_0 fit parameter, $1.58 \pm 0.02 \text{ a.m.u.}$ for $dN_{ch}/d\eta$ and $2.52 \pm 0.2 \text{ a.m.u.}$ for $dE_T/d\eta$ produce a very distinct behavior of the ratio $\langle dE_T/d\eta \rangle / \langle dN_{ch}/d\eta \rangle$ shown in fig. 4. The

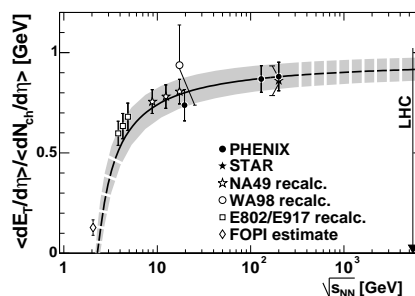


Fig. 4. $\langle dE_T/d\eta \rangle / \langle dN_{ch}/d\eta \rangle$ vs. $\sqrt{s_{NN}}$. Curve is the ratio of the fits discussed in the text.

ratio agrees well to the experimentally measured points and has two different regimes. At low $\sqrt{s_{NN}}$ energy of produced particle

increases with the incident energy. Above $\sqrt{s_{NN}} \approx 10 \text{ GeV}$ incident energy contributes to the number of produced particles, while their energy grows much slower. If the same trend preserves at LHC energies one would expect the ratio to increase only by 5% compare to the highest RHIC energy. Since the $\langle dE_T/d\eta \rangle / \langle dN_{ch}/d\eta \rangle$ is closely related to the freeze-out temperature the LHC freeze-out conditions are expected to be similar to RHIC.

4. Centrality profile

The amount of matter available in a given collision mentioned in the previous section is usually related to the number of participating nucleons N_p . Since this relation is model dependent it was argued since the beginning of RHIC operation whether N_p is an adequate parameter for the event characterization. The answer to this question can be found by comparing PHOBOS data⁹ obtained in $Cu + Cu$ and in $Au + Au$ collisions shown in fig. 5. The $dN_{ch}/d\eta$ well agrees between $Cu + Cu$ and $Au + Au$ events everywhere besides in the Fragmentation regions when one selects collisions with the same N_p . The centrality bins correspond to the most central events in $Cu + Cu$ (impact parameter $b \approx 2 \text{ fm}$) and to about $\sim 40\%$ central in $Au + Au$ ($b \approx 9 \text{ fm}$).

Use of N_p allows to study the centrality behavior of global observables in a quantitative way. All four RHIC experiments provide consistent⁶ results for $dN_{ch}/d\eta$ centrality at mid-rapidity as a function of N_p . PHOBOS experiment uses the same functional form to fit its results measured at several RHIC energies. This is shown in fig. 6.

The magnitude of the curve is different at different $\sqrt{s_{NN}}$ according to the logarithmic trend as it was discussed above. The shape of the curve as a function of N_p remains the same at all energies and well consistent with the data as one can see from

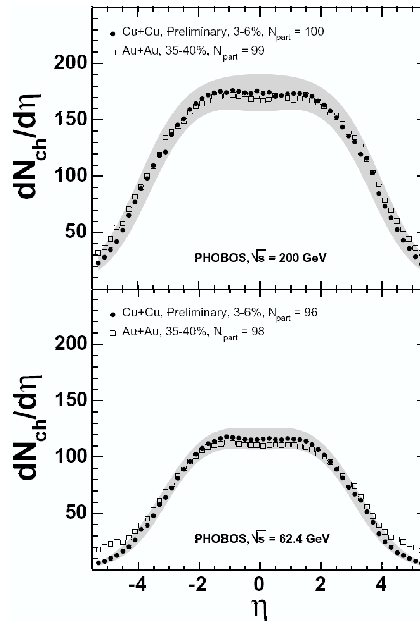


Fig. 5. $Cu + Cu$ and $Au + Au$ data at two RHIC energies selected in centrality bins with the same N_p .

the data to fit ratio in the lower panel in the figure. PHENIX⁶ and STAR⁷ exper-

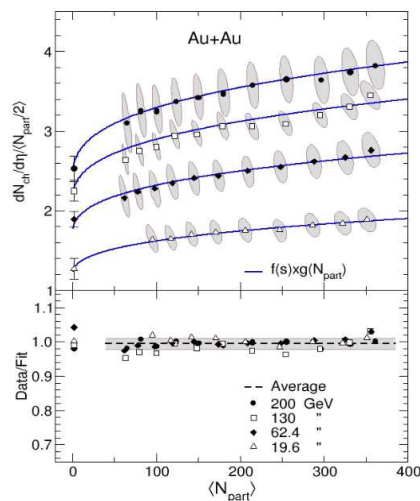


Fig. 6. Mid-rapidity $dN_{ch}/d\eta$ per pair of N_p at different RHIC energies measured by PHOBOS and fitted with the same functional form (top). Data divided by the fit (bottom).

iments measured centrality dependence of the transverse energy production at RHIC.

4

$dE_T/d\eta$ follows closely the shape of the $dN_{ch}/d\eta$ such that the centrality profile of ratio $\langle dE_T/d\eta \rangle / \langle dN_{ch}/d\eta \rangle$ is practically flat, see fig. 7.

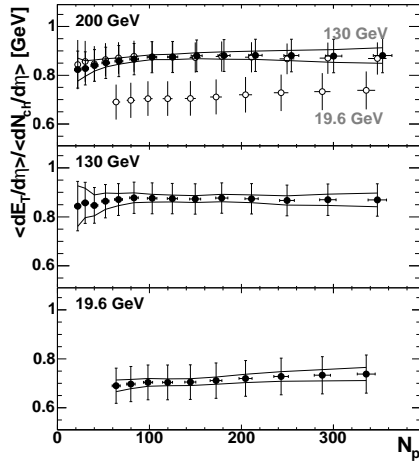


Fig. 7. $\langle dE_T/d\eta \rangle / \langle dN_{ch}/d\eta \rangle$ vs. N_p .

Total particle production over full pseudo-rapidity range exhibits quite different centrality behavior than $dN_{ch}/d\eta$ at mid-rapidity. PHOBOS data⁹ are shown in fig. 8. For all measured centralities it remains constant and $\sim 20\%$ higher than the $p + p$ (and $d + Au$) at the same incident energy.

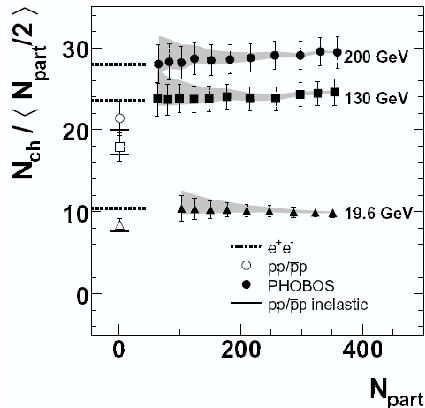


Fig. 8. Total N_{ch}/N_p vs. N_p .

In spite of a successful proof of the N_p validity demonstrated in fig. 5 it still remains a

model dependent quantity. In recent work¹⁰ instead of the number of nucleon participants, the number of quark participants is considered as a parameter to study the centrality dependence. The result is shown in fig. 9. As one can see instead of a rise of

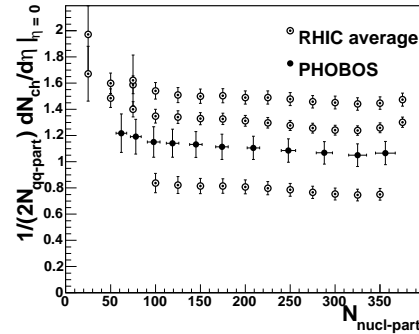


Fig. 9. Mid-rapidity $dN_{ch}/d\eta$ per pair of participating quarks vs. number of participating nucleons.

$dN_{ch}/d\eta$ per nucleon participant shown in fig. 6, the same per quark participants remains flat over all measured centralities.

Work of the speaker is supported by the Goldhaber Fellowship at BNL with funds provided by Brookhaven Science Associates.

References

1. B.B. Back *et al.*, *Phys. Rev. Lett.* **91**, 052303 (2003).
2. P. Staszal *for the BRAHMS Collaboration*, *Nucl. Phys.* **A774**, 97c-92c (2006).
3. R. Noucier *for the PHOBOS Collaboration*, nucl-ex/0601026
4. G.J. Alner *et al.*, *Zeit. für. Phys.* **C33**, 1 (1986).
5. A. Milov, *for the PHENIX Collaboration*, *Nucl. Phys.* **A698**, 171c-176c (2002).
6. S.S. Adler *et al.*, *Phys. Rev.* **C71**, 034908 (2005).
7. J. Adams *et al.*, *Phys. Rev.* **C70**, 054907 (2004).
8. W. Reisdorf *et al.*, *Nucl. Phys.* **A612**, 493 (1997).
9. G. Roland *for the PHOBOS Collaboration*, *Nucl. Phys.* **A774**, 113-128 (2006).
10. S. Volosin and S. Eremin, *Phys. Rev.* **C67**, 064905 (2003).